Original citation:
Schiller, Tara L., Keddie, D. J., Blakey, I. and Fredericks, P. M.. (2016) Surface-enhanced
Raman encoded polymer stabilized gold nanoparticles : demonstration of potential for use in
bioassays. European Polymer Journal.
doi: http://dx.doi.org/10.1016/j.eurpolymj.2016.08.032

Permanent WRAP URL:
http://wrap.warwick.ac.uk/81416

A note on versions:
The version presented here may differ from the published version or, version of record, if
you wish to cite this item you are advised to consult the publisher's version. Please see the
'permanent WRAP url' above for details on accessing the published version and note that
access may require a subscription.

For more information, please contact the WRAP Team at: wrap@warwick.ac.uk

warwick.ac.uk/lib-publications

Surface-enhanced Raman encoded polymer stabilized gold nanoparticles: demonstration of potential for use in bioassays

T. L. Schiller,[a,b*] D. J. Keddie,[c] I. Blakey,[d,e] and P.M. Fredericks[a*]

The preparation of biotinylated, self-assembled polymer stabilized gold nanoparticle hybrids encoded with a SERS active compound is described. The polymers used for nanoparticle stabilization are carefully designed for this purpose and are synthesized by the RAFT polymerization process, as the thiocarbonylthio end group provides a functional handle for anchoring the polymers to the gold surface. Functionalized biotin moieties are attached to the hybrid nanoparticles via Cu-catalyzed azide-alkyne cycloaddition. Binding of the biotinylated hybrid nanoparticles to streptavidin was confirmed by nanoparticle detection and identification by the SERS spectrum of the surface-bound SERS active compound, quinoline thiol. This investigation includes the requisites that constitute a bioassay, demonstrating the potential of polymer-coated hybrid nanoparticles for this purpose.

Introduction

Fluorescence labelling has found considerable use for detection of binding events in bioassays due to its inherent sensitivity and ease of implementation.[1] However, due to broad intrinsic band widths, the number of analytes in an assay is limited. Fluorescence labelling also has other inherent problems, including autofluorescence of the substrate, photobleaching of the dyes, and the need to use multiple excitation sources.[2-4] An alternative strategy for bioassays is based on gold nanoparticles (AuNPs), with surface enhanced Raman spectroscopy (SERS) as the detection technique. SERS has the potential for greater specificity than fluorescence and does not suffer from the obstacles noted above.[2-5] The narrow bandwidths associated with the SERS technique (~20 cm^{-1}) provides the potential to achieve much greater levels of multiplexing than is possible with fluorescence, significantly improving the prospects for increased assay throughput. Recently, a number of papers have reported the use of AuNPs labelled with a SERS active compound (SAC) for use in protein bioassays.[2-7] The function of the SAC is to detect and also differentiate between different AuNPs and has been likened to a "molecular barcode". The use of NPs brings its own problems, the most important of which is the poor long-term stability of the NP suspensions. Our strategy to overcome this has been to prepare SAC-encoded AuNPs stabilized by RAFT polymers,[8] through surface binding of the polymer to Au via the thiocarbonylthio group.[9-19]

Here we demonstrate a model bioassay in which binding to a streptavidin substrate is detected by SERS. This was achieved through the synthesis of polymer stabilized AuNPs functionalized with a biotin moiety, introduced through the polymer end-group. A schematic of this strategy is given in Figure 1. Whilst biotinylated polymer-stabilized AuNPs have been previously in the literature,[17] with turbidity of the solution used to detect a binding event to avidin, detection of the event by SERS as described herein provides more definitive proof of bioconjugation.

There are a number of approaches for the synthesis of polymers with defined architecture; one of the most successful in recent years has been the reversible addition-fragmentation chain transfer (RAFT) process.[18, 19] RAFT polymerization is applicable to a wide range of monomers and, under appropriate conditions, produces polymers with controlled molecular weight and low dispersity. These properties are brought about by use of a thiocarbonylthio chain transfer (or RAFT) agent.[20] A feature of RAFT polymerization is the conservation of the thiocarbonylthio functionality as the ω-end-group in the final polymer (see **Scheme 1**). This provides a functional handle in which to incorporate additional functionality.[21, 22] The polymers were designed to have one end-group ('ZCS2') to specifically bind to the surface of the AuNPs, pendant polyethyleneglycol (PEG) chains, which exhibit low non-specific binding and the α-end-group ('R' group) carries an alkyne functionality, amenable to the Cu-catalyzed click reaction, which can be used to attach biologically active moieties required for bioassays.
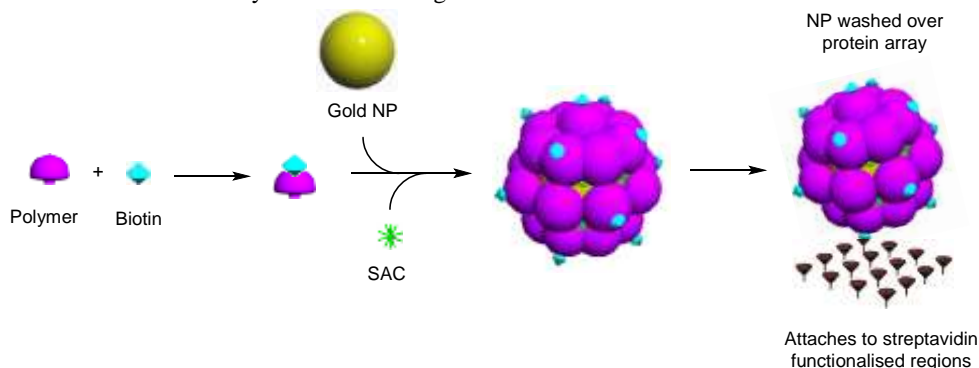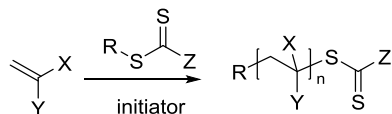

Figure 1: Schematic showing the assembly of hybrid NPs for use in bioassays with SERS detection

Scheme 1: Generic scheme for RAFT polymerization

Results and discussion

For the assembly of the hybrid nanoparticles, we targeted the synthesis of a polymer containing poly(ethylene glycol) (PEG) pendant groups through the RAFT polymerization of PEG methacrylate (PEGMA), because PEG is both water soluble and inhibits non-specific binding to proteins.[23]

RAFT Agent Synthesis

To introduce alkyne functionality in the polymer end-group, we prepared prop-2-ynyl 2-phenyl-2-(phenylcarbonothioylthio)acetate (**5**), bearing the secondary benzylic propargyl ester 'R' group in moderate yield over two steps. Benzylic esters[24, 25] allow for simple introduction of end-group functionality whilst delivering control over the polymerization of methacrylic monomers.[22, 23] Esterification of α-bromophenylacetic acid **1** with propargyl alcohol using DCC coupling gave the bromo ester **2** in 37 % yield (see Scheme 2). Subsequent reaction with benzodithioate salt **4** (prepared from PhMgBr **3** and CS2) gave the alkyne functional dithiobenzoate RAFT agent **5** in 38 % yield.

Scheme 3). The presence terminal acetylene unit is evident through ^{1}H NMR. This functional group readily undergoes a regioselective reaction with azide functionalized molecules via a copper-catalyzed azide-alkyne cycloaddition. (CuAAC).[20]
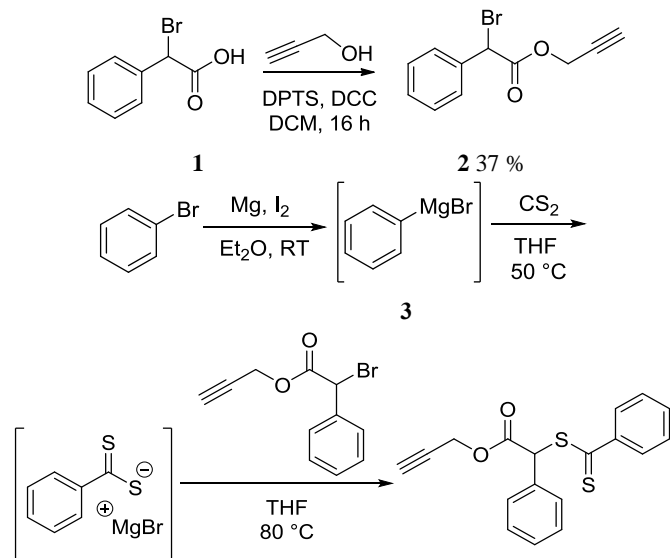
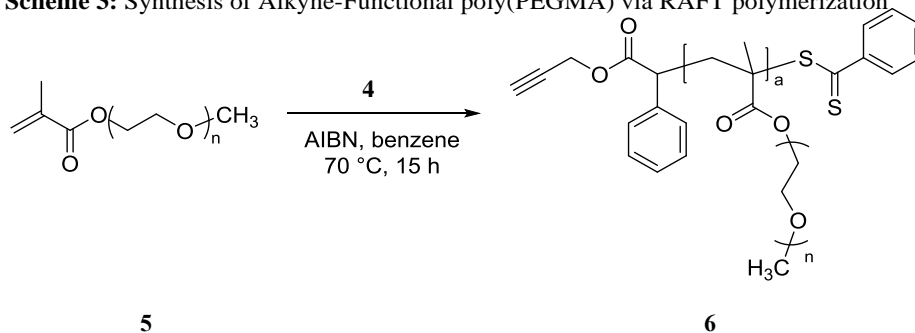### Synthesis of Azido-Functional Biotin

To facilitate functionalization of the polymer with a biotin

4   **2**   **4** 38 %

moiety, the synthesis of an azido-functionalized biotin analogue was undertaken. For this purpose, 4-(5-azidopentyl)tetrahydro-1H-thieno[3,4-d]imidazole-2(3H)-one (**12**) can be synthesized from readily available d-biotin **8** (see Scheme 4). Fischer esterification of d-biotin[27] **8** provides the ethyl ester **9** in high yield (74 %). Subsequent reduction with diisobutylaluminium hydride (DIBAL)[27] furnished the alcohol, biotinol **10** in 71 % yield. Attempted tosylation in anhydrous pyridine resulted in a mixture of the tosylate **11a** (19 %) and chloride **11b** (16%) (35 % combined yield). This appearance of the chloro species **11b** in the reaction of biotinol with sulfonyl chlorides has been previously observed by Islam et al.[28] In this report the treatment of biotinol with methanesulfonyl chloride gave both the mesylate and chloride. Use of excess pyridine in the tosylation reaction, in our case by its use as solvent, can facilitate formation of chloro species by reaction of the pyridinium chloride by-product with the newly formed tosylate.[29] Nevertheless, nucleophilic substitution of this mixture **11** with NaN3 in DMF delivered the requisite biotin azide **12** in moderate yield (62 %) (see Scheme 4 for synthetic route). This compound was then used to create the biotinylated polymer.

Scheme 2: Synthesis of Alkyne-Functional RAFT Agent 4

Scheme 3: Synthesis of Alkyne-Functional poly(PEGMA) via RAFT polymerization

5   6

Scheme 4: Synthesis of Azido-Functional Biotin **12**

7   **8** 74 %

9 71 %   **10a** R= OTs, 19 %   **11** 62 %

10b R = Cl, 16 %
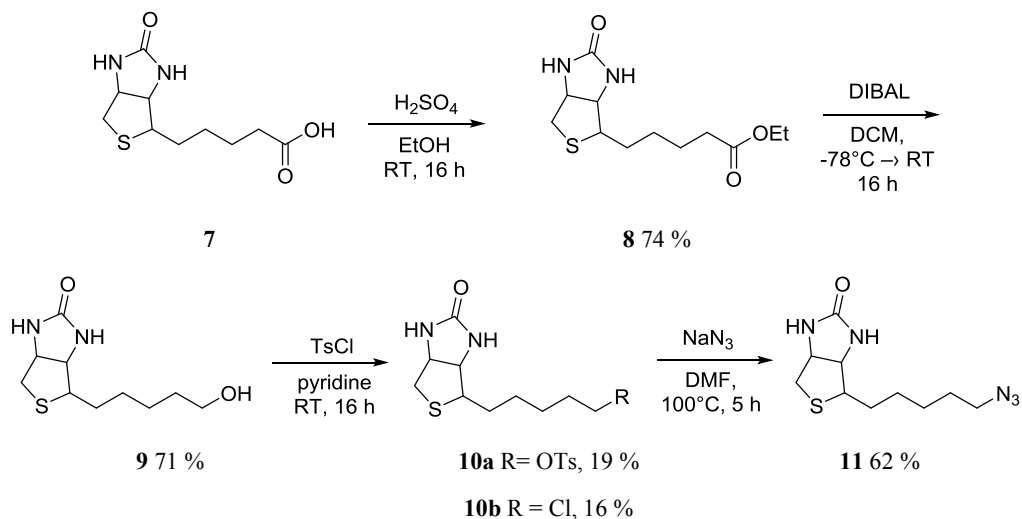
Polymer-Biotin Conjugation via "Click" Chemistry

Successful coupling of the biotin azide **12** to the alkynyl functional (poly)PEGMA **7** was achieved via CuAAC (Scheme 5). The progress of the reaction could be observed by a colour change from a pale pink (the colour of the polymer brought about the chromophore of the RAFT end group) to a dark brown, due to a change in oxidation state of the Cu (II) to Cu (0) (from disproportionation of Cu(I)). The reaction was monitored for completion using ATR-IR spectroscopy, which clearly showed the complete loss of the distinctive azide stretching band near 2100 cm^{-1} (see Figure 2). Note the band appearing at 3200 cm^{-1} is due to the water present. Purification of the biotinylated polymer **13** was achieved by centrifugation of the reaction mixture, removal of the supernatant and resuspension, which was performed in triplicate. The final centrifugation step provided the purified polymer as aqueous solution.
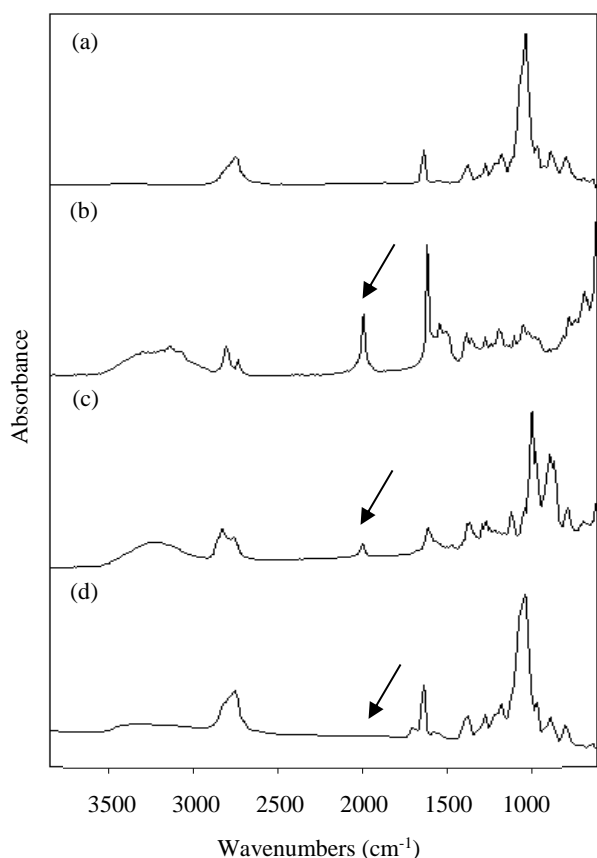
Scheme 4: Polymer-Biotin Conjugation via CuAAC

12
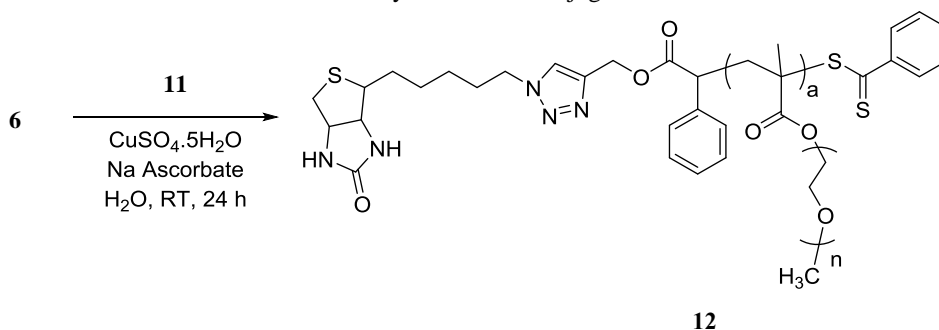
Figure 2: ATR-IR spectra of (a) poly(PEGMA) **6** (b) biotin azide (12) (c) initial reaction mixture of biotin azide **11** and poly(PEGMA) **7** and (d) reaction mixture of **6** and **11** after 2h. The disappearance of the azide peak at 2089 cm^{-1} is noted by the arrow.

Self-Assembly of Biotinylated Polymer Stabilised AuNPs and Tagging with SAC

The self-assembly of the hybrid NPs was achieved by addition of the aqueous solution of biotinylated polymer **13** from above into an aqueous citrate stabilized AuNPs solution. The resulting polymer stabilized AuNPs could be subsequently phase transferred into chloroform, as reported previously,8 for simplified isolation. Importantly, this method allows the phase transfer of hydrophilic AuNPs after their encapsulation by a more hydrophobic polymer, without the addition of a phase transfer agent, allowing for the easy removal of citrate and other unwanted contaminants. The hybrid AuNPs were isolated from chloroform by removal of solvent and resuspended in water. Addition of the SAC, 2-quinolinethiol (QSH) to the aqueous solution resulted in the QSH tagged AuNPs. Successful polymer encapsulation of the AuNPs can be seen in the TEM micrograph (see Figure 3).

Stability Assessment of Hybrid AuNPs

The stability of the polymer-stabilized hybrid AuNPs was assessed by a comparison between alkyne functional polymer hybrid AuNPs and citrate-stabilized AuNPs after addition of saturated sodium chloride (NaCl) solution. NaCl is expected to destabilize AuNPs because of the rapid change in solubility of the nanoparticles.
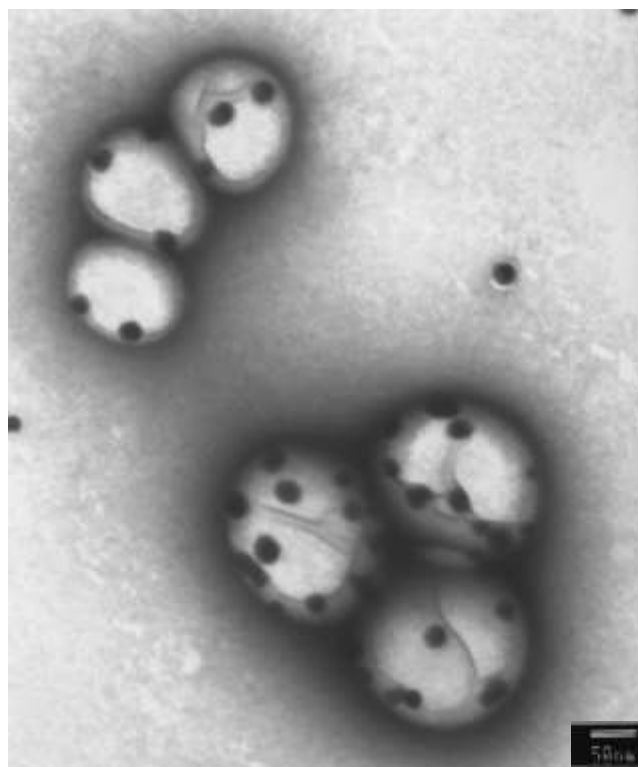
Figure 3: Representative TEM micrograph image of polymer stabilised AuNPs

The citrate stabilized AuNPs showed complete destabilization on addition of NaCl, indicated by a colour change from bright pink/purple in solution to black (a sign of aggregation) immediately after the NaCl addition. Within a few minutes the now aggregated AuNPs precipitated leaving a black film on the bottom of the vessel. The presence of a colourless supernatant indicated the absence of AuNPs in solution. An example of irreversible aggregation is show in Figure S3 in the supporting information. In stark contrast, the addition of NaCl solution did not affect the stability of hybrid AuNPs; that is no colour change was observed and no change in the surface Plasmon resonance (SPR) was detected by visible spectroscopy. These observations illustrate that the hybrid AuNPs have considerably enhanced stability compared to citrate stabilized AuNPs.

Bioconjugation of Streptavidin

Due to the remarkable binding affinity of biotin to streptavidin,[21] the interaction between this protein-ligand pair has become a commonly used method of bioconjugation.[22] To illustrate the

potential of polymer stabilized NPs for use as detection modalities in bioassays, SERS detection of a binding event between streptavidin and the biotinylated hybrid AuNPs was undertaken. As streptavidin possesses several biotin binding sites, the AuNPs were expected to precipitate from solution following the addition of the streptavidin. Whilst precipitation was observed experimentally, this did not provide definitive proof a binding event had taken place. Alternatively the aggregation may be due to the presence of a salt or another destabilizing agent.

Since we required further evidence of detection of the biotin streptavidin binding to illustrate the viability of our AuNP system for bioassay application, an assay where streptavidin is surface-bound (an ELISA-like assay)[23] was also undertaken. For this process a solution of the biotinylated AuNPs was washed over a streptavidin functionalized surface. The surface was subsequently washed with water to remove any AuNPs adsorbed to (but not bound to) the surface. Binding was confirmed by SERS. AuNPs without biotin conjugation was compared as a negative control.

Figure 3 shows the SERS spectra of the RAFT end-group (a) the SAC 2-quinolinethiol (b), and the Raman spectrum of polystyrene well plate (c). It can be seen that the SERS spectrum obtained from the well plate after treatment with the hybrid AuNPs (Figure 3 (d)) contains bands around 790, 1080, 1330 and 1380 cm-1 which accord well with the SERS spectrum of the SAC, 2-quinolinethiol (Figure 3(b)). There were also additional bands, such as the intense band near 1000 cm-1 together with weaker bands at 1050, 1210 and 1600 cm-1, which correspond well with the SERS spectrum of the RAFT group. We have recently shown that related phenyldithioesters interact strongly with the AuNP surfaces through the C=S bond RAFT endgroup.31 In the spectrum shown in Figure 3 (a), the intense band near 1000 cm-1 can be assigned to the ring breathing mode of the aromatic ring, while the less intense bands at 1050, 1210 and 1600 cm-1 can be assigned to υC-S, υC=S and the C=C stretch of the aromatic ring, respectively. Additional contribution obtained from the polystyrene substrate can also be observed in the SERS spectrum of the biotin-streptavidin surface bound AuNPs (Figure 3 (d)).

The binding experiment described above was repeated using hybrid NPs which were composed of PEGMA which had not been biotinylated, but did incorporate the SAC, 2-quinolinethiol. After washing the well plate in the same way the Raman spectrum did not reveal any bands due to the hybrid AuNPs, either from the SERS spectrum of the RAFT end-group, or from the SAC. This indicated that, as expected, in the absence of the biotin moiety there is no binding to the immobilized streptavidin and the hybrid AuNPs were removed from the well during the washing procedure.

Whilst the SERS spectrum of the bound hybrid AuNPs contains bands due to the polystyrene substrate, the existence of the SERS spectrum of the SAC is clear. At least four significant bands can be seen and their positions uniquely identify both the presence and identity of the hybrid AuNPs.

In order to further illustrate that the binding event occurred, confocal Raman microscopy was employed to examine the change in intensity of the SERS signal of both the SAC and the

RAFT agent, in comparison to the polystyrene substrate. The SERS spectra at varying depths of laser penetration are shown in Figure 4, with the peaks arising from each analyte labelled in the same fashion as for Figure 3 (RAFT = R; quinolinethiol = Q; polystyrene = PS; labels are shown above the top spectrum only for clarity). The SERS spectrum of the surface bound NPs, measured at the laser focus depth that gave maximum signal
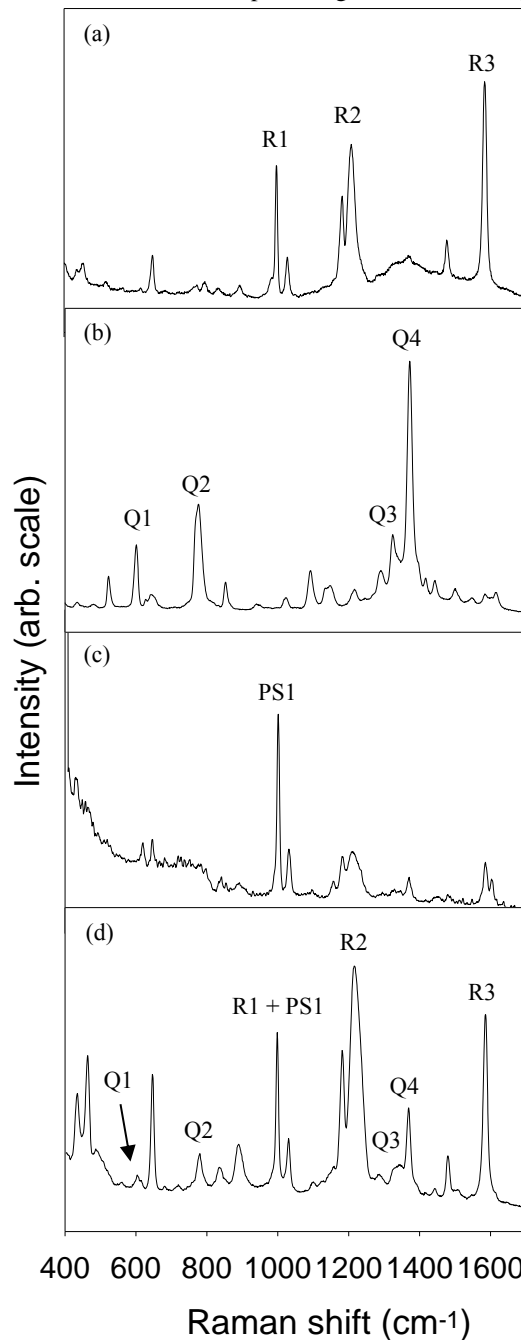

Figure 3: SERS spectra of (a) RAFT end group of **13**, (b) 2-quinolinethiol, (c) Raman spectrum of the well plate's polystyrene substrate, and (d) the SERS spectrum after the binding event; the major peaks corresponding to the RAFT end-group of **13**, 2-quinolinethiol and polystyrene substrate are

labelled as R, Q and PS respectively and numbered for ease of correlation.

intensity for the SAC and RAFT agent peaks is shown in Figure 4 (a). When the depth of focus of the laser was varied from this position, then the signal intensity varied. As the depth of focus was moved 50 µm toward the substrate the PS peak at 1000 cm-1 (PS1) becomes more prominent, indicated by a change in the relative peak intensity compared to the peak arising from the RAFT group at approximately 1200 cm^{-1} (R2) (see Figure 4 (b)). The bare PS substrate is shown for comparison in Figure 4 (c).

The change in relative intensity of the peaks at 1000 cm-1 and 1200 cm-1 suggests there is a contribution to the signal at 1000 cm-1 arising from the PS substrate. In spite of this, the SERS signals from the RAFT group and the SAC are easily observed in Figure 4 (a) and clearly illustrate successful binding of the biotinylated AuNPs to the streptavidin functionalized surface.

These results illustrate the potential utility of our SERS detected hybrid AuNP system for use in both precipitation and ELISA-like surface bound assays. The advantages of each assay type can be exploited through their use: (a) the simplicity of precipitation assays and (b) the sensitivity of the ELISA/surface binding method.

Conclusions

In summary, we have synthesized biotinylated polymer-stabilized hybrid AuNPs incorporating a SAC, 2-quinolinethiol. This material interacts strongly with streptavidin immobilized on a polystyrene surface and this binding can be detected by the SERS spectrum of the SAC. Binding to streptavidin was not observed for hybrid AuNPs which did not contain the biotin moiety, and no SERS spectrum was observed. The sequence of reactions discussed in this paper constitutes a bioassay and hence demonstrates the potential for hybrid AuNPs, using tailored polymers, to be used as a novel approach to bioassays, with SERS as the detection method. The illustration of this procedure in multiplexing experiments will be the focus of future investigations.

Experimental

Materials: Unless otherwise stated, all reagents and solvents were used as received. All water used was MilliQ Ultrapure 18 MΩ cm. SigmaScreen™ Streptavidin High Capacity Coated Plates and all chemicals were purchased from Sigma Aldrich, with the exception of streptavidin and biotin that were purchased from Anaspec.

Characterization: [1]H Nuclear Magnetic Resonance (NMR) spectra were collected using a 5 mm BBOz gradient probe at 298 K on the Bruker Avance 300 MHz and ^{13}C spectra were collected using a 5mm SEIz probe at 298K on the Bruker Avance 400 MHz. Deuterated solvents for NMR spectroscopy were commercially obtained (Cambridge Isotopes) and were of 99.8 atom % D. Chemical shifts (δ) are reported in parts per million (ppm) relative to residual solvents.[24] Gel permeation chromatography (GPC) measurements of the polymers were performed using a Waters Alliance 2690 Separations Module equipped with an autosampler, column heater, differential refractive index detector and a Photo Diode Array (PDA) connected in series. HPLC grade tetrahydrofuran was used as the eluent at a flow rate of 1 mL min^{-1}. The columns consisted of three 7.8 x 300 mm Waters Styragel SEC columns connected in series, comprising of two linear Ultrastyragel and one Styragel HR3 columns. Polystyrene standards ranging from 2000000-517 g mol^{-1} were used for calibration and all GPC derived molecular weights are quoted in polystyrene equivalents. Raman spectra were recorded with a Renishaw
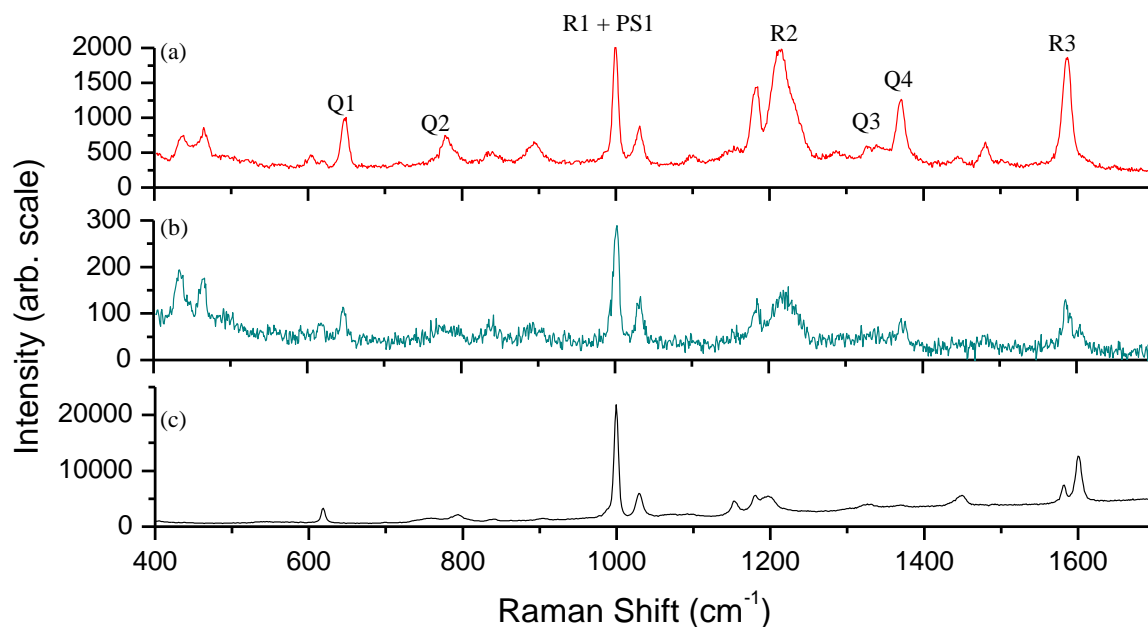
Figure 4: Depth profile confocal Raman microscopy spectra measured at (a) the depth of maximum Raman peak intensity, (b) 50 μm toward the substrate from the point of maximum signal intensity, and (c) the polystyrene substrate.

Model 1000 micro Raman spectrometer (Renishaw plc, Wotton-under-Edge, UK) equipped with a 785 nm excitation source from a diode laser, a single diffraction grating and an electrically cooled CCD detector. A 10 % neutral density filter was used, which resulted in a laser power at the sample of about 1 mW. A single accumulation in the spectral range 2000–200 cm^{-1} was collected for each sample. Confocal mode with a pinhole inserted was used for measurements taken on the streptavidin well plate. Transmission Electron Microscopy (TEM) micrographs were imaged on a JEOL 1200 TEM, where the energy was set to 80 kV and spot size 3. Solutions of citrate AuNPs in water and solutions of polymer stabilised AuNPs in chloroform were dropped onto carbon-celloidin coated 200-mesh copper TEM grids and allowed to dry before placing in TEM sample holder. Citrate stabilised AuNPs that were dispersed in water, were synthesised using the citrate method.[25, 26] Size of the nanoparticles was confirmed on a Joel 1200 TEM. TEM micrographs of AuNPs synthesised by the citrate method were analysed and average size was taken. Samples were mounted on celloidin – carbon coated 200 mesh copper grids. It should be noted that the NPs aggregated on the carbon coated TEM grids during sample preparation. Attenuated Total Reflectance - Fourier Transform Infrared (ATR-FTIR) spectra were obtained on a Nicolet Nexus 5700 FTIR spectrometer equipped with a Nicolet Smart Orbit single bounce, germanium ATR accessory (Thermo Electron Corp., Waltham, MA). Spectra were recorded at 4 cm^{-1} resolution for at least 32 scans with an OPD velocity of 0.6289 cm s^{-1}. Solids were pressed directly onto the Ge internal reflection element of the ATR accessory without further sample preparation. Spectra were manipulated using the OMNIC 7 software package (Thermo Electron Corp., Waltham, MA).

Synthesis of prop-2-ynyl 2-phenyl-2-(phenylcarbonothioylthio)acetate (acetylene RAFT agent, 4)

Part 1: Esterification reaction (synthesis of prop-2-ynyl 2-bromo-2-phenylacetate, 2)

Propargyl alcohol (1.21 g, 21.62 mmol, 1 equiv) was dissolved in DCM (12.5 mL). α-Bromophenylacetic acid (5.58 g, 25.93 mmol, 1.2 equiv) and 4-(dimethylamino)pyridinium 4-toluenesulfonate (DPTS) (1.27 g, 4.32 mmol, 0.2 equiv) were then added to the solution. *N,N*'-Dicyclohexylcarbodiimide (DCC) (6.69 g, 32.40 mmol, 1.5 equiv) was dissolved in a separate flask in DCM (12.5 mL) and then transferred slowly to the reaction vessel. Upon addition of the DCC, the reaction mixture became cloudy as DCC urea was produced. The reaction was stirred overnight at room temperature under Ar to ensure completion, after which the reaction mixture was filtered to remove the precipitate. The DCM solvent was removed under vacuum leaving an oily yellow residue. This was purified by column chromatography (SiO$_2$, eluent: *n*-hexane) to give the desired propargyl ester **2** as a clear, colourless oil (1.97 g, 8.0 mmol, 37 %); ^{1}H NMR (400 MHz, CDCl3) δ ppm 2.54 (1H, t, J = 2.3 Hz, C≡CH), 4.76 (1H, dd, J = 2.3 and 15.3 Hz, HCHC≡CH), 4.82 (1H, dd, J = 2.3 and 15.3 Hz, HCHC≡CH), 5.42 (1H, s, CBrH), 7.34-7.44 (3H, m, ArH), 7.54-7.61 (2H, m, ArH), ^{13}C NMR (100 MHz, CDCl3) δ ppm 45.9 (alkyl C), 53.7 (alkyl C), 75.8 (C≡C), 76.5 (C≡C), 128.6 (ArC), 128.8 (ArC), 129.4 (ArC), 135.1 (ArC), 167.5 (C=O)

Part II: Synthesis of acetylene RAFT agent (prop-2-ynyl 2-phenyl-2-(phenylcarbonothioylthio)acetate, 4)

Phenyl magnesium bromide (PhMgBr), was prepared by placing pre-dried magnesium (0.561 g, 23.38 mmol, 3 equiv) and a couple of small crystals of iodine in a 50 mL oven-dried two-neck round-bottomed flask. The flask was then attached to a Schlenk manifold via a reflux condenser. The flask was flame-dried under high vacuum, resulting in a fine coating of iodine on the magnesium. The vessel was then placed under argon for the remainder of the reaction.

Et$_2$O (dried over Na wire) (10 mL) was added to the reaction vessel. Subsequently, bromobenzene (0.99 mL, 1.47 g, 9.35 mmol, 1.2 equiv) was added dropwise ensuring the reaction occurred at a constant rate. When the addition was complete, the reaction was stirred until all activity subsided. The solution of Grignard reagent, PhMgBr, was then quantitatively transferred in a dry, gas-tight syringe to a clean oven-dried 3-neck flask, attached to a reflux condenser.

Subsequently, dry THF (20 mL) was added to the PhMgBr solution. CS$_2$ was added drop wise using a dry glass syringe and needle, and the solution became dark red-brown. After the addition was complete, the reaction was heated to 50 °C for 30 min to ensure full conversion. A solution of prop-2-ynyl 2-bromo-2-phenylacetate (1.98 g, 7.79 mmol, 1 equiv) in dry THF (20 mL) was then added to the reaction vessel. The flask was covered with Al foil to minimize degradation of the product by light and stirred at 80 °C for 15 hours and subsequently the solvent was removed under vacuum. Purification by column chromatography (50% CHCl$_3$/50% *n*-hexane) gave the acetylene RAFT agent **4** as a red oil (0.92 g, 2.81 mmol, 38 %); FT-IR ATR (cm^{-1}): 2920, 1691, 1588, 1463, 1443; ^{1}H NMR (400 MHz, CDCl3) δ ppm 2.52 (1H, t, J = 2.3 Hz, C≡CH), 4.73 (1 H, dd, J = 2.3 and 15.3 Hz, HCHC≡CH), 4.84 (1 H, dd, J = 2.3 and 15.3 Hz, HCHC≡CH), 5.77 (1H, s, SCHPh), 7.36-7.61 (8H, m, ArH), 8.00-8.06 (2H, m, ArH) ^{13}C NMR (100 MHz, CDCl$_3$) δ ppm 53.6 (alkyl C), 58.6 (alkyl C), 75.7 (C≡C), 76.9 (C≡C), 127.0 (ArC), 128.5 (ArC), 128.9 (ArC), 129.1 (ArC), 129.2 (ArC), 132.6 (ArC), 132.9 (ArC), 143.8 (ArC), 168.2 (C=O), 225.7 (C=S).

Synthesis of poly(PEGMA) 6 using the acetylene RAFT agent 4

The acetylene RAFT **4** agent was used to synthesize a PEGMA polymer by RAFT polymerization as follows: Poly(ethylene glycol) methacrylate **5** (M_n=475, PEGMA) (3 g, 6.32 mmol) was weighed into a Schlenk flask, then benzene (3.3 g) was added. 2,2'-Azobisisobutyronitrile (AIBN) (12.9 mg, 0.078 mmol) was added to the flask, along with the RAFT agent **4** (257.1 mg, 0.789 mmol) ([PEGMA]:[RAFT]:[AIBN] = 8:1:0.1). The mixture was purged under argon for approximately 15 minutes then sealed and placed in an oil bath at 70 °C for 15 h. Crude samples were taken from the mixture and characterized by NMR and GPC analysis to ascertain full monomer conversion and molecular weight. The resulting polymer was dissolved in a small amount of DCM and purified by precipitation into cold diethyl ether. The ether was then removed by decantation to give the polymer **6** as a pink gum. Further NMR and GPC analysis of the polymer **6** confirmed the removal of the starting materials (NMR in Figure S1 and S2 of the supporting information); (GPC: M_n = 7800, M_w = 8600, M_w/M_n = 1.10).

Synthesis of 4-(5-Azidopentyl)tetrahydro-1H-thieno[3,4-d]imidazole-2(3H)-one 11

Synthesis of Ethyl [(3aS,4S,6aR)-2-oxo-hexahydro-thieno[3,4-d]imidazol-4-yl]pentanoate (8)

Biotin **7** (1.0 g, 4.09 mmol) was dissolved in absolute ethanol (25 mL) and the resulting solution was acidified by adding several drops of conc. H_2SO_4. The reaction mixture was stirred at room temperature for 16 h, after which the volatiles were removed under reduced pressure. The crude product was taken up in DCM (50 mL), and washed with saturated $NaHCO_3$ (3 × 30 mL) and H_2O (2 × 30 mL). The organic layer was dried (Na_2SO_4) and the solvent was removed under reduced pressure to give a white solid. Recrystallisation from cold acetone gave ethyl [(3aS,4S,6aR)-2-oxo-hexahydro-thieno[3,4-d]imidazol-4-yl]pentanoate (**8**) as a white crystalline solid (0.82 g, 3.01 mmol, 74 %). FT-IR ATR: 3236, 2926, 2861, 1731, 1709, 1478, 1284 cm^{-1}; ^{1}H NMR (400 MHz, CDCl3) δ ppm 6.00 (s, 1H), 5.61 (s, 1H), 4.53-4.43 (m, 1H), 4.32-4.24 (m, 1H), 4.09 (q, J = 7.13 Hz, 2H), 3.25-3.03 (m, 1H), 2.88 (dd, J = 12.80, 4.96 Hz, 1H), 2.71 (d, J = 12.78 Hz, 1H), 2.30 (t, J = 7.50 Hz, 2H), 1.77-1.54 (m, 4H), 1.52-1.33 (m, 2H), 1.23 (t, J = 7.13 Hz, 3H); ^{13}C NMR (100 MHz, CDCl3) δ ppm 173.686, 163.744, 61.931, 60.284, 60.101, 55.443, 40.530, 33.933, 28.328, 28.220, 24.781, 14.232; HRMS mass calculated for $C_{13}H_{23}N_2O_3S^+$: 273.1195 experimental ESI [M+H]$^+$: 273.1273.

Synthesis of 4S-[(3aS,6aR)-5-Hydroxy-pentyl]-tetrahydro-thieno[3,4-d]imidazol-2-one (9)

Biotin ethyl ester **8** (200 mg, 0.733 mmol) was dissolved in DCM (0.7 mL) and placed under argon and cooled to -78 °C (dry ice/acetone). Diisobutylaluminium hydride (DIBAL) (1.72 mL, 2.5 mmol, 1.5 M in toluene) was added dropwise over 10 minutes. The mixture was stirred at -78 °C for a further 20 minutes then allowed to warm to room temperature and stirred for 16 h. The mixture was again cooled to -78 °C and quenched by dropwise addition of methanol, a mixture of methanol and water and finally water. The solvents were removed under reduced pressure and the product was extracted with ethanol using a Soxhlet apparatus. Subsequently the EtOH was removed under reduced pressure to give an off white solid. Purification by column chromatography (50 % EtOAc/50 % EtOH) gave 4S-[(3aS,6aR)-5-hydroxy-pentyl]-tetrahydro-thieno[3,4-d]imidazol-2-one (**9**) as a white solid (119 mg, 0.517 mmol, 71 %); FT-IR ATR: 3244, 2931, 2369, 1700, 1477cm^{-1}; ^{1}H NMR (400 MHz, MeOH-d4 6.62 (s, 1H), 6.58 (s, 1H), 4.56-4.46 (m, 1H), 4.35-4.29 (m, 1H), 3.57 (t, J = 6.50, 6.50 Hz, 2H), 3.27-3.19 (m, 1H), 2.95 (dd, J = 12.76, 4.98 Hz, 1H), 2.72 (d, J = 12.72 Hz, 1H), 1.91 (s, 1H), 1.83-1.35 (m, 1H); ^{13}C NMR (100 MHz), MeOH-d4 ppm 161.7, 62.0, 61.5, 55.8, 39.6, 33.5, 32.0, 28.8, 28.4, 25.5. HRMS mass calculated for $C_{10}H_{19}N_2O_2S^+$: 231.1089 experimental ESI [M+H]$^+$: 231.1167. These data were found to have some discrepancy compared with those reported in literature.[27, 28] It is suggested that some of the NMR data may have been misreported as the product reported in literature was not purified after the Soxhlet extraction.

Synthesis of 4S-[(3aS,6aR)-5-(4-toluenesulfonyl)pentyl]-tetrahydro-thieno[3,4-d]imidazol-2-one (10a) (4S-[(3aS,6aR)-5-chloropentyl]-tetrahydro-thieno[3,4-d]imidazol-2-one (10b))

Biotinol **9** (119 mg 0.57 mmol) was dissolved in warm anhydrous pyridine (2.5 mL) under argon. This solution was cooled in an ice bath for 30 minutes after which *p*-toluenesulfonyl chloride (120 mg, 0.63 mmol, 1.1 equiv.) was added. After stirring at 0 °C for 5 minutes the reaction mixture was allowed to warm to RT and was stirred for a further 16 h. The mixture was poured into cold water (~50 mL) and extracted with DCM (3 × 50 mL). The DCM solutions were then washed with 1.8 M H_2SO_4 (3 × 50 mL). The aqueous layers were extracted with additional DCM (2 × 150 mL). The DCM layers were combined and subsequently washed with brine (3 × 100 mL) and dried over Na_2SO_4. The solvent was removed and the obtained solid was purified by column chromatography (1:20 MeOH:DCM). NMR and MS characterisation of the obtained product indicated the presence of both tosyl **10a** and chloro **10b** functionalised biotin (60 mg, 19 % **10a**, 16 % **10b** (concentrations from NMR), 0.2 mmol, 35 % overall yield). Further attempts to separate these proved unsuccessful and the mixture was used in subsequent steps without additional purification.

Tosylate **10a** ^{1}H NMR (400 MHz, CDCl3) δppm 7.79 (d, 2H, J=8.1 Hz), 7.36 (d, J=8.1 Hz, 2H), 6.34 (s, 1H), 5.65 (s, 1H), 4.56-4.50 (m, 1H), 4.03 (t, J = 6.4 Hz, 2H), 3.22-3.07 (m, 1H), 2.94-2.87 (m, 1H), 2.76 (d, J = 5.7 Hz, 1H), 2.46 (s, 3H), 1.83-1.30 (m, 8H); ^{13}C NMR (100 MHz, CDCl3) δ ppm 163.9, 144.7, 133.0, 129.8, 127.8, 77.2, 70.6, 60.0, 55.6, 28.5, 28.3, 28.3, 25.3, 21.6; HRMS calculated for tosylate $C_{17}H_{24}N_2O_4S_2$: 384.12 experimental ESI [M+H]$^+$: 385.1256;

Chloride **10b** ^{1}H NMR (400 MHz, CDCl3) δ ppm 6.05 (s, 1H), 5.73 (s, 1H), 4.36-4.30 (m, 1H), 3.54 (t, J = 6.7 Hz, 2H), 3.22-3.07 (m, 1H), 2.96-2.87 (m, 1H), 2.73 (d, J = 5.7 Hz, 1H), 1.54-1.31 (m, 8H); ^{13}C NMR (100 MHz, CDCl3) δppm 163.8, 61.9, 60.0, 55.5, 45.0, 40.5, 32.2, 28.4, 28.2, 26.7; HRMS calculated for chloride $C_{10}H_{17}N_2SOCl$: 248.0750 experimental ESI [M+H]$^+$: 249.0828. These data agree with both biotin tosylate and biotin chloride.[27, 29]

Synthesis of 4-(5-Azidopentyl)tetrahydro-1H-thieno[3,4-d]imidazole-2(3H)-one 11

To the biotin tosylate/chloride mixture **10** (60 mg, 0.2 mmol) and sodium azide (32 mg, 0.6 mmol, 3.2 equiv.) was added to DMF (0.5 mL). The resultant solution was heated at 100 °C for 5 hours. The reaction mixture was cooled and water was added forming a white precipitate. Filtration of the precipitate gave 4-(5-azidopentyl)tetrahydro-1H-thieno[3,4-d]imidazol-2(3H)-one **11** (30 mg, 0.117 mmol, 62 %) mp: 85 °C; FTIR ATR showed a characteristic azide peak at 2100 cm^{-1}; (400 MHz, CDCl3) δ ppm 1.55-1.36 (m, 4H), 1.85-1.57 (m, 8H), 2.76 (d, J = 12.81 Hz, 1H), 2.95 (dd, J = 12.84, 5.05 Hz, 1H), 3.22-3.15 (m, 1H), 3.29 (t, J = 6.83, 6.83 Hz, 2H), 4.38-4.29 (m, 1H), 4.57-4.50 (m, 1H), 5.21 (s, 1H), 5.47 (s, 1H); ^{13}C NMR (100 MHz, CDCl3) δ ppm 163.3, 62.1, 60.1, 55.5, 51.4, 40.6, 28.6, 28.6, 26.7; HRMS mass calculated for $C_{10}H_{18}N_5OS^+$: 256.1154 experimental ESI [M+H]$^+$: 256.1232.

Gold Nanoparticle Synthesis

Gold nanoparticles were prepared as we reported previously,[8] via adaption of the method reported by Grabar *et al*.[30]

Briefly, an aqueous solution of chloroauric acid ($HAuCl_4$) (100 mL, 1.0 mM) was heated to boiling, after which an aqueoussolution of sodium citrate (3.5 mL, 38.8 mM) was added. To ensure complete reduction, the solution was boiled for a further 15 min. The reaction

was cooled to room temperature and stored as an aqueous suspension of AuNPs. All characterization data was consistent with that reported previously.[8]

Polymer Biotin Conjugation

The copper-catalyzed azide-alkyne cycloaddition (CuAAC) was first performed in water to test the reaction, since it is reported to proceed more readily in aqueous media. Both ^{1}H NMR and FTIR-ATR were used to monitor the disappearance of the azide functionality. These reactions were performed with an excess of the acetylene coupling partner (in this case the PEG homopolymer **2**) to ensure complete conversion of the azide.

Preparation of biotin functionalized AuNPs: CuAAC of hybrid gold polymer nanoparticle with biotin azide.

The poly(PEGMA)**12** (74 mg) was dissolved in 1 mL water. Biotin azide **11** (1.1 mg) was added to the vial, from an 11 mg/1 mL solution. The reagents were made up to 1 mL each (13 mg $CuSO_4 \cdot 5H_2O$ and 16 mg of sodium ascorbate respectively) into water so that 100 µL could be added to the vial and the reaction(s) stirred for 24 hours. Purification was conducted by centrifugation.

Approximately 1mL AuNPs solution was placed in a clean vial. The biotin polymer product (100 µL) was added to the AuNPs and followed approximately 60 seconds later by 5, 10 or 200 µL of a 54 µM solution of 2-quinolinethiol (QSH) and the resultant mixture was stirred overnight, to allow the QSH to penetrate into the polymer. The reaction was monitored for completion using ATR-IR with a Ge crystal.

Approximately 1 mL of AuNP solution was placed in 10 separate vials, so that reproducibility could be ascertained. Poly(PEGMA)**12** (35 mg) was dissolved in water (10 mL). Subsequently, 0.5 mL of the polymer solution was added to the AuNP vial. This was shaken and then set aside for an hour to allow attachment of the polymer to the nanoparticle surface. Stability of the AuNPs was assessed by the addition of NaCl to a vial of the hybrid AuNPs (not incorporating biotin) and to a vial of citrate stabilised AuNPs.

Demonstration of binding to streptavidin.

The SigmaScreen™ Streptavidin High Capacity Coated Plates were obtained from Sigma Aldrich. The AuNP/biotin-conjugate polymer **12** solution (200 µL, as prepared) was added to each well on the well plate. The well plates were left to rest at RT for at least 2 hours and then washed vigorously with PBS and 5 % tween 20 to remove any unbound material. SERS was used to analyse the presence of a signal to indicate the binding event.

The biotin was added to a well plate that had been pre-treated with streptavidin. Instructions supplied by Sigma with the well plate meant that approximately 200 µL of the AuNP/biotin solution needed to be added to individual wells on the well plate. This was left at RT for at least 2 hours then washed vigorously with PBS (phosphate buffered saline) and 5 % tween 20 (mild surfactant). The streptavidin solutions for this study were prepared at a concentration of 5×10^{-6} M in 0.5 M aqueous NaCl.

The SERS signal of solution and plate was examined before and after washing. Control samples were also analysed, using AuNPs with a SERS tag but no biotin attached. Wells were prepared using the above procedure except without any biotin present.

Notes and references

[a] Chemistry, Faculty of Science and Technology, Queensland University of Technology, Brisbane, Queensland 4000, Australia.

[b] Warwick Manufacturing Group, University of Warwick, Coventry CV47AL, UK.

[c] School of Biology, Chemistry and Forensic Science, University of Wolverhampton, Wolverhampton, WV1 1LY, UK

[d] Australian Centre for Advanced Imaging, University of Queensland, St Lucia, Queensland 4072, Australia.

[e] Australian Institute for Bioengineering and Nanotechnology, University of Queensland, St Lucia, Queensland 4072, Australia.

1. K. D. Kumble, *Analytical and Bioanalytical Chemistry*, 2003, **377**, 812-819.
2. W. E. Doering and S. Nie, *Analytical Chemistry (Washington)*, 2003, **75**, 6171-6176.
3. D. S. Grubisha, R. J. Lipert, H.-Y. Park, J. Driskell and M. D. Porter, *Analytical Chemistry (Washington)*, 2003, **75**, 5936-5943.
4. S. P. Mulvaney, M. D. Musick, C. D. Keating and M. J. Natan, *Langmuir*, 2003, **19**, 4784-4790.
5. M. D. Porter, R. J. Lipert, L. M. Siperko, G. Wang and R. Narayanana, *Chemical Society Reviews*, 2008, **37**, 1001.
6. Y. C. Cao, R. Jin, J.-M. Nam, C. S. Thaxton and C. A. Mirkin, *Journal of the American Chemical Society*, 2003, **125**, 14676-14677.
7. S. Xu, X. Ji, W. Xu, X. Li, L. Wang, Y. Bai, B. Zhao and Y. Ozakic, *Analyst (London)*, 2004, **129**, 63.
8. Z. Merican, T. L. Schiller, C. J. Hawker, P. M. Fredericks and I. Blakey, *Langmuir*, 2007, **23**, 10539-10545.
9. M. Beija, J.-D. Marty and M. Destarac, *Chemical Communications (Cambridge, United Kingdom)*, 2011, **47**, 2826-2828.
10. M. Beija, E. Palleau, S. Sistach, X. Zhao, L. Ressier, C. Mingotaud, M. Destarac and J.-D. Marty, *J. Mater. Chem.*, 2010, **20**, 9433-9442.
11. S. Sistach, M. Beija, V. Rahal, A. Brulet, J.-D. Marty, M. Destarac and C. Mingotaud, *Chem. Mater.*, 2010, **22**, 3712-3724.
12. M. Beija, J.-D. Marty and M. Destarac, *Progress in Polymer Science*, 2011, **36**, 845-886.
13. I. C. Lin, M. Liang, T.-Y. Liu, Z. M. Ziora, M. J. Monteiro and I. Toth, *Biomacromolecules*, 2011, **12**, 1339-1348.
14. M. Liang, I. C. Lin, M. R. Whittaker, R. F. Minchin, M. J. Monteiro and I. Toth, *ACS Nano*, 2010, **4**, 403-413.
15. C. Boyer, M. R. Whittaker, K. Chuah, J. Liu and T. P. Davis, *Langmuir*, 2010, **26**, 2721-2730.
16. J. Liu, E. Setijadi, Y. Liu, M. R. Whittaker, C. Boyer and T. P. Davis, *Australian Journal of Chemistry*, 2010, **63**, 1245-1250.
17. P. Dey, S. Zhu, K. J. Thurecht, P. M. Fredericks and I. Blakey, *Journal of Materials Chemistry B*, 2014, **2**, 2827-2837.

18. P. Dey, I. Blakey, K. J. Thurecht and P. M. Fredericks, *Langmuir*, 2014, **30**, 2249-2258.

19. P. Dey, I. Blakey, K. J. Thurecht and P. M. Fredericks, *Langmuir*, 2013, **29**, 525-533.

20. H. C. Kolb, M. G. Finn and K. B. Sharpless, *Angewandte Chemie*, 2001, **40**, 2004-2021.

21. T. R. Ward, *Accounts of Chemical Research*, 2010, **44**, 47-57.

22. R. Sunasee and R. Narain, in *Chemistry of Bioconjugates*, John Wiley & Sons, Inc., 2014, pp. 1-75.

23. J. Chen and G. C. Howard, in *Making and Using Antibodies* eds. G. C. Howard and M. R. Kaser, CRC Press, Foster City, CA, USA, 2 edn., 2014, pp. 385-394.

24. H. E. Gottlieb, V. Kotlyar and A. Nudelman, *J. Org. Chem.*, 1997, **62**, 7512-7515.

25. G. Frens, *Nature*, 1973, **241**, 20.

26. W. S. Sutherland and J. D. Winefordner, *Journal of Colloid and Interface Science*, 1992, **148**, 129.

27. C. Corona, B. K. Bryant and J. B. Arterburn, *Org. Lett.*, 2006, **8**, 1883-1886.

28. P. J. DeLaLuz, M. Golinski, D. S. Watt and T. C. Vanaman, *Bioconjugate Chem.*, 1995, **6**, 558-566.

29. I. Islam, K.-y. Ng, K. T. Chong, T. J. McQuade, J. O. Hui, K. F. Wilkinson, B. D. Rush, M. J. Ruwart, R. T. Borchardt and J. F. Fisher, *Journal of Medicinal Chemistry*, 1994, **37**, 293-304.

30. K. C. Grabar, R. G. Freeman, M. B. Hommer and M. J. Natan, *Analytical Chemistry*, 1995, **67**, 735-743.